



## Using artificial neural networks for predicting flood events in Artvin, Türkiye

Olgu Aydın <sup>\*1</sup>, Nussaibah Begum Raja <sup>2</sup>

<sup>1</sup> Ankara University, Faculty of Language, History and Geography, Department of Geography, Türkiye, oaydin@ankara.edu.tr

<sup>2</sup> GeoZentrum Nordbayern, Friedrich-Alexander-Universität Erlangen-Nürnberg, Erlangen, Germany, nussaibah.raja.schoob@fau.de

Cite this study: Aydın, O., & Raja, N. B. (2025). Using Artificial Neural Networks for Predicting Flood Events in Artvin, Türkiye. Turkish Journal of Engineering, 9 (2), 189-201.

<https://doi.org/10.31127/tuje.1530593>

### Keywords

Rainfall  
Flood Forecasting  
Artificial Neural Network (ANN)  
Early Warning Systems  
Artvin

### Research Article

Received:08.08.2024  
Revised:23.09.2024  
Accepted:28.09.2024  
Published:01.04.2025



### Abstract

Flood risks in Artvin, Turkey, have become a critical concern due to the long-term economic, social, cultural, and environmental damages caused by flood-related disasters. Given this, it is essential to utilize reliable methods for flood prediction. Artificial Neural Networks (ANNs), adept at reacting to rapid changes in rainfall, are employed as a machine learning approach to provide valuable flood information for urban areas. This study aims to develop an accurate and timely flood prediction model for Artvin using daily average rainfall data from 58 weather stations between 2009 and 2016. Flow values for various locations in Artvin (Ardanuç, Arhavi, Artvin, Borçka, Hopa, Murgul, Şavşat, Yusufeli) are calculated using the rational method. ANNs were trained with daily rainfall data and consecutive rainfall inputs from 1 to 7 hours to predict flow values. The model's performance, with 75% of the data used for training and 25% for validation, showed an error ratio of 0.225 and high prediction accuracy for flow values, exceeding 20 m<sup>3</sup>/h in most locations except Hopa. The R<sup>2</sup> results for 1–7 hours indicated high performance (0.643-0.725), suggesting effective warning times of 3–5 hours for Artvin. The study also highlights the increasing necessity for flood management strategies in the Eastern Black Sea Region, particularly Artvin, which has experienced severe flash floods and significant flooding events since 2017. The region's frequent and intense rainfall, exacerbated by global climate change, underscores the urgent need for robust monitoring, early warning systems, and comprehensive flood mitigation plans to address drainage, land management, and safeguard infrastructure. Effective warning systems that provide real-time estimates of rainfall and flow are crucial for timely preventive measures.

## 1. Introduction

Flood-related disasters, which compose 40% of all disasters that happen in the world [1-2], occur in different regions of world and affect people negatively as well as cause loss of life and property [3]. Residential areas, human safety and well-being, health and nutrition, water and sanitation, education, agriculture, and infrastructure can all be disrupted or damaged, affecting the basic needs and services of the affected population [4]. The flood occurring in the Arno River Basin in Italy caused an economic loss of 15.5 billion Euros [5]. Between 1959 and 2005, there were 4.586 fatalities in the United States attributed to flood events. The years with high numbers of fatalities coincided with floods caused by tropical systems or sudden flash floods [6]. Furthermore, 6.8 million people lost their lives in the flood-related disasters during the 20th century [7]. Out of these, 50% of these casualties occurred in the Asian countries, only in the last quarter of the 20th century [7].

In Turkey, the frequency of meteorologically-induced disasters has been increasing every year, with floods and inundations being among the most frequently encountered incidents. In their study, Gürer and Uçar [8] determined that approximately 3250 flood events were recorded in the flood inventory analysis for the period 1955–2020. When evaluating the spatial distribution of these events, the Black Sea Region, Eastern Anatolia, and the Mediterranean Region are identified as having high flood risk. When examining flood events that occurred between 1948 and 2023 in Turkey, it was determined that the highest number of flood events, based on regions and subtypes of floods, occurred in the Black Sea Region [8]. Since 1948, the total economic damage caused by floods in Turkey has exceeded 2.793 billion US dollars [9]. Taking all these assessments into account, the global impacts of floods are negative, and their increase is expected to continue as long as climate change persists [10].

Flash flood events are caused by heavy rainfall, as a result of storms and hurricanes. Small temporal and spatial scales on which these flash floods occur make it difficult to observe and predict these sudden events [11]. With this in mind, factors such as the construction of monitoring and early warning systems, the formulation of preparatory plans, the establishment of a community based defense system, dissemination of flood control information and training are becoming a necessity [12-13]. An effective warning system allows enough time to take necessary preventive measures, by making real time estimation of rainfall or flow values prior to the flood event [14]. Through evacuation measures, the risks that can endanger human life are thus minimized. For this purpose, many countries have attempted to predict flood disasters. For example, flood warnings in the United States are provided by comparing the rainfall amount with Flash Flood Guidance (FFG) values [15]. The Bureau of Meteorology in Australia has introduced a flash flood warning system called ALERT that is capable of detecting floods in large and small river basins, sending warning messages to authorities if rainfall intensity or flow level criteria are exceeded [16]. In the Rungkut region of Indonesia, an Internet of Things (IoT)-based flood disaster early detection system has been successfully implemented, seamlessly integrated with social media, enabling residents to access the latest information on flood conditions and ensuring a safer and more comfortable environment [17]. The Machine Learning (ML), Artificial Neural Network (ANN) has been among the most commonly used methods in recent studies on flash flood events [18, 19, 20, 21-22]. Çubukçu et al. [23] stated that there are more than 48 research articles in the Scopus database utilizing ANN models for maximum flow forecasting. Byaruhanga et al. [24] found in their study conducted using Scopus and Web of Science electronic databases that time series models (TSMs) were the most frequently used models for flood prediction between 1993 and 2010. However, they identified that ML models, especially ANNs, have been the dominant models from 2011 to the present day. ANN is able to predict possible future flood events by using flow and rainfall information [25]. Many studies have previously used ANNs to estimate flood flow values, e.g. Çubukçu et al. [23], Campolo et al. [26], Artigue et al. [27], Cools et al. [28], Raja and Aydin [29], Lamsal and Vijay Kumar [30] and others. These studies have consistently shown that the performance of neural network models improves significantly with larger datasets. This enhancement in model performance allows early warnings to be issued within a few hours, which is crucial for effective disaster preparedness and response [31]. Early warning systems thus provide timely alerts, enabling decision-makers to take proactive measures such as evacuating residents from disaster-prone areas [30].

Artvin has been chosen as an important area for flood studies due to its location in Turkey's Eastern Black Sea Region and its high flood risk. The four major flash flood events that occurred between 2015 and 2017 highlight the seriousness of the flood risk in the region. The region usually experiences high-intensity rainfall events that lead to flash floods and landslides [32]. Artvin's

geographical and climatic conditions, combined with its socio-economic activities, make it particularly vulnerable to flooding. The city relies heavily on agriculture and forestry, sectors that can exacerbate the impact of floods. Artvin has experienced a series of significant flooding events since 2017. The process began with a severe flood in Arhavi in July 2018, followed by a major flood in Yusufeli in July 2020, and another severe rainfall-induced flood in Arhavi in July 2021. In September 2022, Arhavi faced another flooding event, and in October 2023, widespread floods occurred in Arhavi, Borçka, and Hopa regions. The recurrent nature of these floods underscores the ongoing challenges related to drainage, land management, and the need for comprehensive flood mitigation strategies to safeguard the local population and infrastructure. The irregularity in the rainfall regimes, attributed to global climate change, has caused sudden and heavy rains, increasing the risk of flooding in cities [33]. It is becoming a key necessity to take precautions against flood risk and to minimize its damages given the long-term economic, social, cultural and environmental damages due to flood-related disasters in the city of Artvin. The aim of this study is to develop a flash flood forecasting system, so as to take the necessary measures in the city of Artvin, where the risk of flooding is high. For this purpose, the artificial intelligence-based ANN method was utilized. The study presents an innovative approach to flood forecasting in Artvin that has not been used before. Additionally, it evaluates flood risks using comprehensive meteorological data from 2009 to 2016, allowing for the analysis of long-term trends. By considering the unique geographical and climatic conditions of Artvin, the study develops locally applicable solutions and contributes to regional disaster management. These elements highlight the contributions of the study to scientific literature and practical applications, offering an innovative perspective. Additionally, it enhances community preparedness against flash flood events, ensuring the safety of local residents and holding the potential to minimize economic losses. In this way, it lays the groundwork for more effective measures to be taken against the increasing flood risks associated with climate change.

## 2. Materials and Method

### 2.1. Study Area

The city of Artvin is located, at northeast of Turkey's Black Sea Region on the border of Georgia, between 40° 34' 19.55"- 41° 31' 29.62" north latitude and 41° 09' 25.41"- 42° 35' 47.16" east longitude (Figure 1). The city of Artvin consists of eight districts, namely Ardanuç, Arhavi, Borçka, Hopa, Merkez, Murgul, Şavşat and Yusufeli (Figure 2). The presence of steep slopes make up the city's important topographic features. Approximately 80% of the city is located over 1000 m above sea level, 31.07% of this ratio covers areas over 2000 m [34]. There are three large mountain groups in Artvin and the surrounding areas: the Eastern Black Sea Mountains, the Mescit Mountains and the Yalnızçam Mountains. The biggest river in the city is the Çoruh River which runs from south to northeast. The most well-known branches

of the Çoruh River are the Barhal Creek in the east, the Murgul and Hatila (Atila) Creek in the southwest. The city of Artvin is located in the North Anatolian orogenic belt. The metamorphic series extending from the lower section of the Çoruh River towards the northeast through Sirya is the oldest area. The largest geological unit of the city is the upper Cretaceous volcanic series and the volcano-sedimentary series. The acid and neutral lavas and their agglomerates and tuffs, as well as red coloured marls and limestone plates in thin beds are included in this series. In addition, dacite, andesite, matches and quartz porphyries are in the series [35, 36-37]. The presence of semi-permeable volcanic rocks in the city is remarkable.

The climate is moist and temperate. Winters are warm, while summers are hot and characterized by frequent heavy rain. Based on the data obtained from the Artvin meteorological station for the years 1949–2004, the annual total rainfall is 689 mm, and the average temperature is 12.2 °C. The lowest rainfall occurs in July (30 mm) and August (28 mm), while the highest average temperature values are 20.6 °C and 20.7 °C, respectively, in the same months [38]. Observations from 2015 highlight significant rainfall events in the region. For example, on August 24, 2015, the Hopa district experienced 30–50 mm of rainfall between 8:00 and 9:00 pm. On November 11, 2015, the Borçka district recorded  $\geq 15$  mm of rainfall at 4:00 pm. Additionally, on November 12, 2015, rainfall lasted for 7 hours, with values ranging between 5 and 10 mm. The study also emphasizes the susceptibility of districts such as Arhavi and Murgul to flash floods [32]. The development of these floods has been influenced by synoptic mechanisms, including warm northerly flows from the Black Sea and cool southerly flows from the land coasts, which contribute to the formation of deep convective cells and subsequent flash floods [39]. After 2015, the annual average total rainfall varied in 2018, 2019, and

## 2.2. Data Collected

In this study, daily average rainfall values obtained from 58 meteorological stations between the years 2009 and 2016 were used. The flood events of 2009 and 2016 were specifically selected due to their significant impacts on the region and the availability of comprehensive data for these years, which enables a detailed analysis of the factors contributing to flooding. The data used in this study was obtained from the General Directorate of

2020. The highest rainfall occurred in 2020. In terms of annual average temperatures, the highest temperature was recorded in 2018, while the lowest temperature was measured in 2020 [40]. Temperature and rainfall are key climatic factors that significantly influence the occurrence and intensity of flash floods. Elevated temperatures can enhance evaporation rates and contribute to the formation of convective storms, while high rainfall levels increase the likelihood of excessive runoff and flash flooding. The region is influenced by the Black Sea with moist air coming from the Çoruh River and the Cankurtaran Passage, and due to its high elevation, frequent rainfall and fog occur.

The steep slopes, low infiltration, and high surface flow in the city lead to landslides after heavy rainfall. Among other factors that trigger floods in Artvin, the location of settlement areas in stream floodplains is particularly significant. Given the city's steep terrain, planting deep-rooted trees is necessary to improve soil retention. However, tea cultivation is a major source of income for the city. Consequently, forest areas are converted into tea gardens, disrupting the natural balance of the land. Hydroelectric Power Plant (HPP) projects have also become popular in Artvin. The city and its districts host 15 dams and 166 river-type HPPs. The environmental damage caused by HPPs cannot be ignored; it disrupts river integrity and leads to habitat fragmentation. The stripping of soil at HPP construction sites deteriorates the natural balance of slopes and causes significant land damage. Rural settlements also lack adequate infrastructure to manage frequent floods and landslides. The discharge of wastewater into septic tanks results in the continuous saturation of the ground around houses. The rapid urbanization of the city, illegal land use, heavy rains from storms in and around Artvin all contribute to flooding and landslide events, leading to severe loss of life and property.

Meteorology. 8 of the meteorological stations are located in Artvin, 19 in Rize, 6 in Ardahan and 25 in Erzurum. Figure 1 shows the distribution of meteorological stations. In addition, the locations where the flow value is calculated are determined as the locations of the meteorological stations in the districts of Artvin (Figure 2). The analyses were carried out using the R 3.1.0 program (Ihaka and Gentleman, Auckland, New Zealand) and the related packages (gstat, rgdal, maptools, geo-R and neuralnet) [41, 42-43].

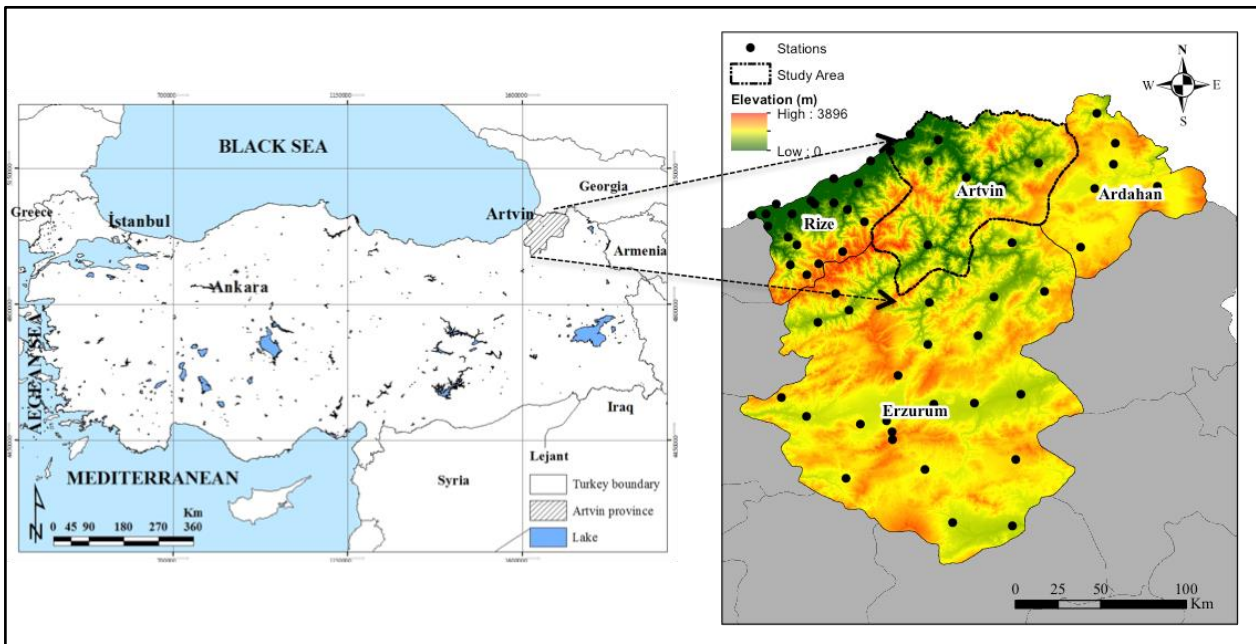


Figure 1. Distribution network of meteorological stations across study area, with “value” refering to elevation (m).

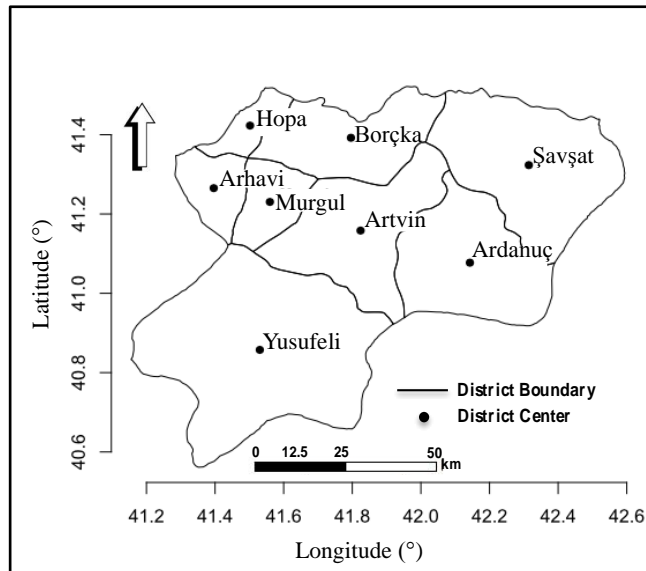


Figure 2. Locations of places where flow value is calculated in Artvin.

### 2.3. Rational method

In flood calculations, the flow value can be used as a variable. Therefore, the flow value used in ANN method is calculated for the above-mentioned locations determined in Artvin. The rational method is preferred for small city basins. It is an empirical linear equation used to calculate the maximum speed of flow. This formula is given in Equation 1.

$$Q = kCiA \quad (1)$$

Here  $Q$ , is expressed as the highest surface flow rate,  $c$ , rational method surface flow coefficient,  $i$ , rainfall density in mm/h, and  $A$ , is expressed as the drainage area in  $\text{km}^2$ . The flow coefficient is the depth of the flow and the total rainfall depth ratio.

$$C = \frac{R}{P} \quad (2)$$

In Equation 2,  $R$  represents the total flow depth,  $P$ , represents total rainfall depth. The flow coefficient refers to the rate at which rainfall is converted to flow. The flow coefficients used in the rational method were calculated using Thompson [44]’s provided values.

### 2.4. Artificial neural network (ANN)

ANN was developed to imitate the human brain through the implementation of mathematical models. It is a system that is inspired by the biological structures in the brain of people who can perform tasks such as information processing, learning and adaptation. The main element of the network structure is the neuron. Three layers of neurons containing different numbers form the most basic structure of the network. The first layer forms the input layer from which the external information is received; the last layer forms the output layer from which the results are obtained. There are

intermediate layers known as hidden layers between the input and output layers. The intermediate layers are used to process the information and send it to the output layer using the weighted values of the network. The efficiency of the ANN model depends on input variables and therefore it should be carefully integrated into the model [45]. Too much input increases the volume of the network structure and extends the training process. The weights indicate the effect of the information on the cell. It is known as a measure of the connection forces of the inputs. The learning function is carried out by changing the weights. The summation function calculates the net inputs from a cell. Mathematically, inputs can be displayed as  $(I_1, I_2, \dots)$  and weights can be displayed as  $(w_1, w_2, \dots)$ . The summation function is obtained by increasing the weight component by each element of the input element.  $(Input1 = I_1 * w_1, Input2 = I_2 * w_2, \dots \sum Input1 + Input2)$ . In short, it is defined as the sum of the inputs multiplied by the related weight. The activation function processes the net input which comes to the cell and determines the output that the cell will generate against this input. Different formulas are used to calculate the output. The function selected as an activation function depends on the data of the neural network and what it wants to learn. In addition, activation functions allow output values to remain within certain limits. The outputs in the network structure are expressed as the output value determined by the activation function [46].

The output of each is obtained by computing the value of the activation function with respect to the product of the input vector and the weight vector, minus the value of the bias associated with that node. A network with one hidden layer and  $K$  outputs can be expressed as shown in Equation 3.

$$f_k(x, y) = w_{k0} + \sum_{j=1}^q w_{kj}g \left( w_{j0} + \sum_{i=1}^p w_{ji}x_i \right) \quad (3)$$

where  $p$  is the number of inputs,  $q$  is the number of nodes in the hidden layer,  $g$  is the activation function of the hidden layer nodes and  $x$  and  $w$  are the weights. The indices  $i$  and  $j$  correspond to the output node and hidden layer nodes, respectively. However, ANNs are rarely expressed as such since the equation is not interpretable.

Before an ANN can be used to perform any desired task, it must be trained. During this process, the weights  $W$  are determined in order to minimise the error between the inputs and the outputs in the training dataset. The formula used in the calculations is given in Equation 4.

$$E_D = \sum_{i=1}^n (t_i - a_i)^2 \quad (4)$$

where  $E_D$  is the sum of the error square between the targets  $t$  and the ANN response  $a$  for  $i$  observations in the input-output dataset. The training input data is in the form of vectors of input variables or training patterns. Each element in an input vector corresponds to an input node in the network input later; therefore the number of input nodes is equal to the dimension of the input vectors, i.e. the number of independent variables. The total available data is divided into a training set, a validation set (75%) and a testing set (25%). The training set is used for estimating the weights whilst the validation set is used to help stop the training process else the ANN may overfit the data and lose its ability to generalise to an unseen dataset. Then the network is tested on an unseen dataset, i.e. the testing set, in order to measure the performance of the network. ANN structure must be tested to see if the error level is within acceptable limits. For this purpose, the process steps are repeated until a low error rate is achieved.

### 3. Results and discussion

Figure 3 shows daily average rainfall between the years 2009–2016. When the graph is examined, the red dots indicate the average daily rainfall values higher than the average. Moreover, it is noteworthy that the average daily rainfall values are at the highest values for 23-09-2009, 24-08-2015, 12-11-2015, 25-08-2016 in which flood disasters occur in the city of Artvin. Using daily average rainfall in ANN model is important because of its usage as input. The locations in which the weather stations are located in the districts of Artvin were determined as the locations where flow values are to be calculated. The reason for this, the flood events in 23-09-2009, 24-08-2015, 12-11-2015, 25-08-2016 affected significantly, particularly Hopa, Arhavi, Borçka, Murgul districts as well as other districts of Artvin City. Damages caused by the floods can be seen in the district center and its vicinity. These locations were defined as input data in the ANN structure. Calculation of the flow value for the locations of meteorological stations in the districts of Artvin constitutes the first step in the analysis. The flow value was calculated by taking into account the daily average rainfall values between the years of 2009–2016. The flow value ( $m^3/h$ ) calculated for the designated locations is defined as the output data in the ANN structure. In addition, time data is another input data defined in ANN structure. Time is the time interval determined to calculate how many hours before the flood event it can be estimated before it occurs.

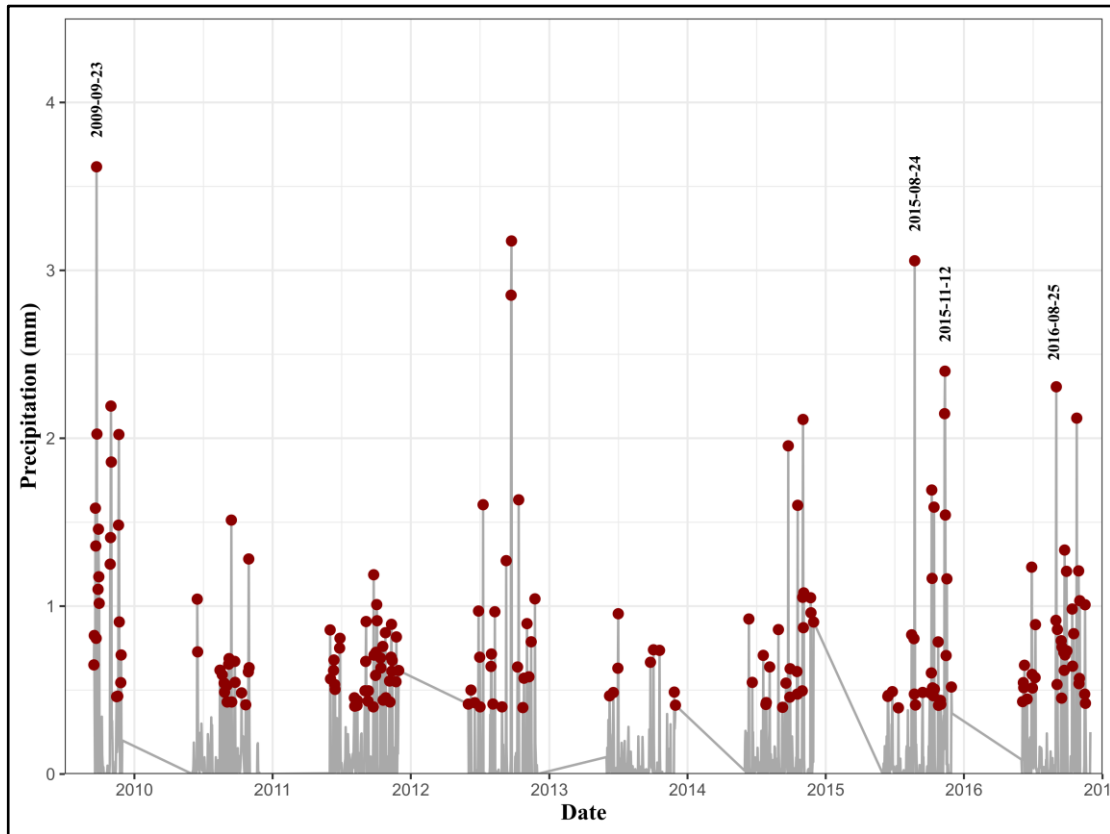


**Figure 3.** Graph showing average daily rainfall values for between the years 2009–2016.

In this case, the inputs were determined as location, rainfall and time. The location is defined in the network structure as a categorised variable. Rainfall is a continuous variable and it forms daily average rainfall values. The time was categorised for the time before the flood event, between 1–7 hours. The network structure consists of 2 hidden layers, with 4 and 2 nodes respectively. The output in the network structure represents the calculated flow value ( $\text{m}^3/\text{h}$ ) for the selected locations. In the structure of the network, 75% of the data is used for training, 25% is for testing. The system was repeated 47,291 times to train the network structure. During the training, the process was repeated until the error rate of 0.225 was obtained. The aim here is to train the network structure until the lowest error rate is achieved. The ANN structure computed during this study is given in Figure 4. The performance result of the model was evaluated. In addition, the performance results were calculated for each hour, for a period of 1 and 7 hours prior to the event happening. Figure 5 shows the state of the observed flow value and the estimated flow value relative to each other. For most locations, the

model reaches a threshold, after which the flow values stagnates, showing that the model is unable to predict values after this threshold is achieved. This threshold value however remains above  $20 \text{ m}^3/\text{h}$ , which suggests that the model is able to predict high flow values and thus is able to predict a potential flood event for these locations. With the exception of Hopa district, all the other districts, namely Ardanuç, Arhavi, Artvin, Borçka, Murgul, Şavşat, Yusueli showed high performance from the model.  $R^2$  values of these districts are above 0.50. The highest values are observed 0.75 for Ardanuç and 0.74 for Borçka. The reason for the very low estimation for the district of Hopa is that the behaviour of the small basins is different. Instead of creating a model for the whole work area, it would be more appropriate to create a separate model for Hopa. Moreover, Hopa district is one of the districts most affected by floods. The joint evaluation of other special characteristics of this area may lead to high estimation results.

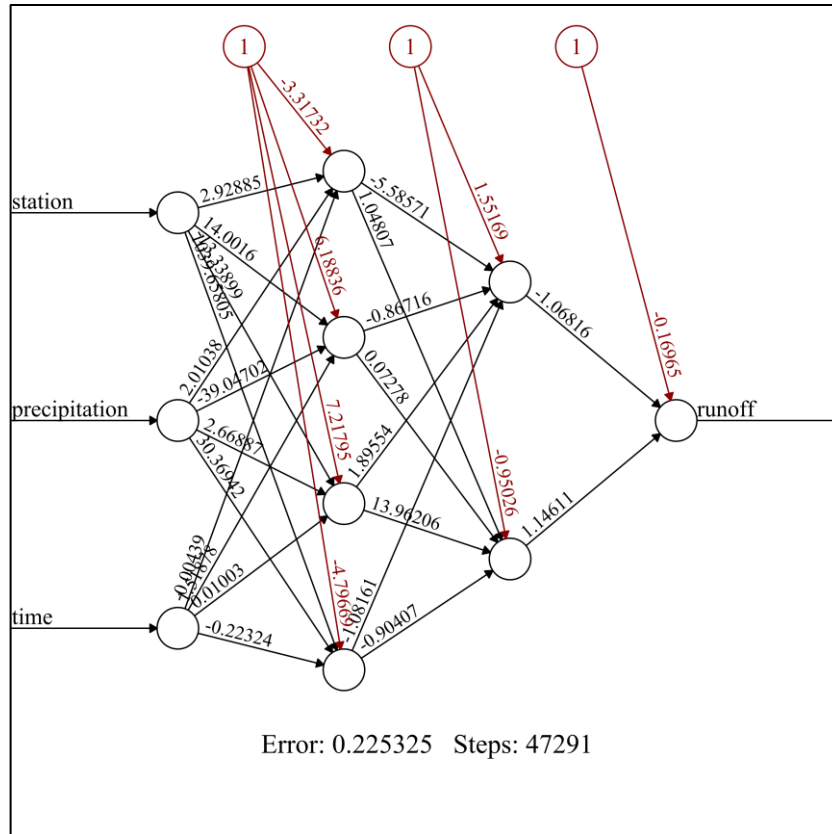


**Figure 4.** Artificial Neural Network (ANN) structure in the study.

Figure 5 shows the state of the observed flow value and the estimated flow value relative to each other. For most locations, the model reaches a threshold, after which the flow values stagnates, showing that the model is unable to predict values after this threshold is achieved. This threshold value however remains above 20 m<sup>3</sup>/h, which suggests that the model is able to predict high flow values and thus is able to predict a potential flood event for these locations. With the exception of Hopa district, all the other districts, namely Ardanuç, Arhavi, Artvin, Borçka, Murgul, Şavşat, Yusueli showed

high performance from the model. R<sup>2</sup> values of these districts are above 0.50. The highest values are observed 0.75 for Ardanuç and 0.74 for Borçka. The reason for the very low estimation for the district of Hopa is that the behaviour of the small basins is different. Instead of creating a model for the whole work area, it would be more appropriate to create a separate model for Hopa. Moreover, Hopa district is one of the districts most affected by floods. The joint evaluation of other special characteristics of this area may lead to high estimation results.

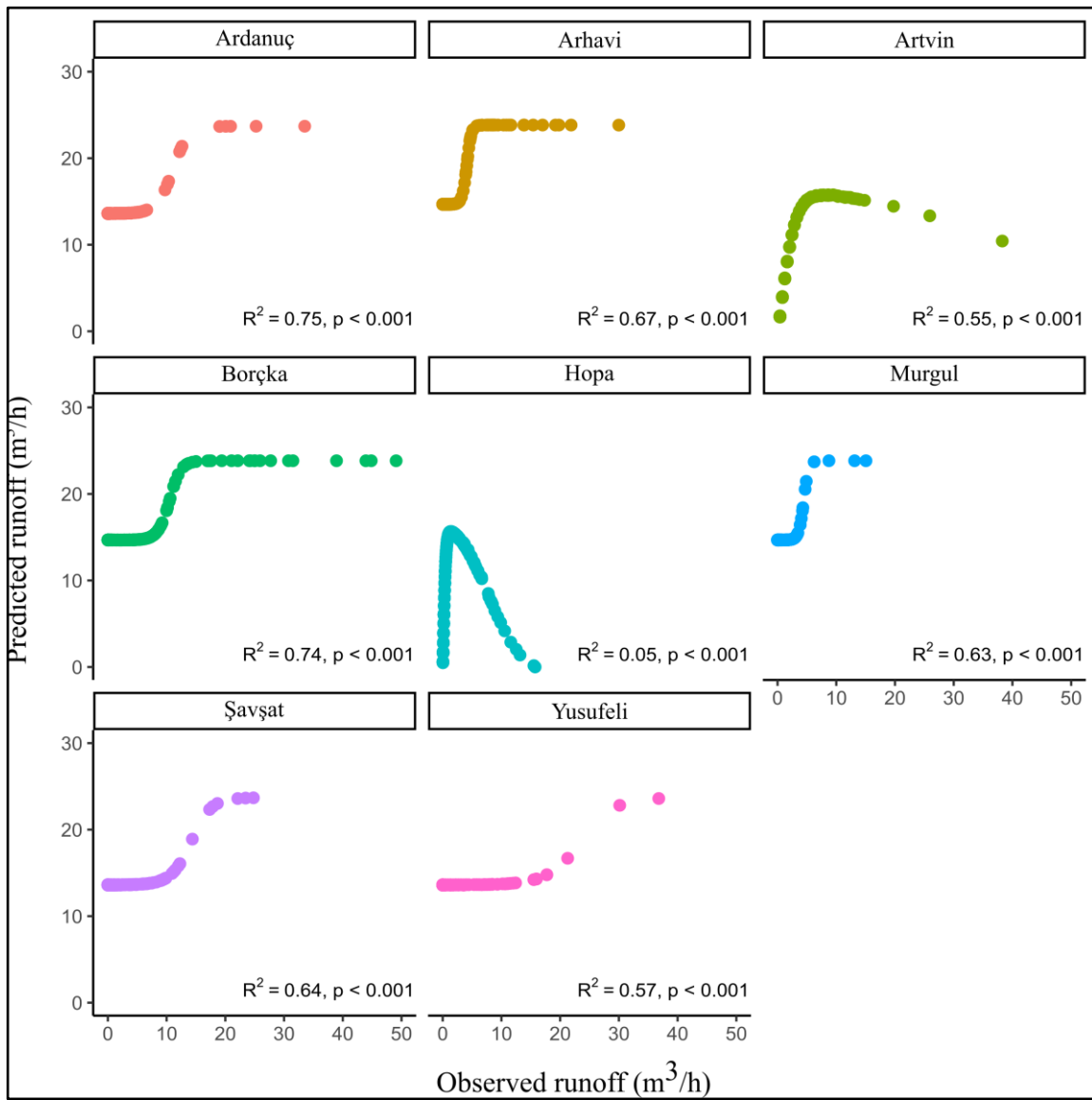


**Figure 5.** Graphical representation of estimated and observed flow values in locations determined in the city of Artvin.

The results of the performance measurements for 1–7 hours period before the flood event is provided in Table 1. Accordingly, the  $R^2$  performance values for the time periods of 3–5 vary between 0.643-0.759.

Table 2 shows the times of concentration for each location. These were 3 hours for Borçka, Şavşat and Arhavi districts. According to this, it can be stated that the times of the concentrations for the Artvin districts range between 3 and 5 hours.

**Table 1.** Performance results for 1–7 time interval for floods.

Performance Measurements	$L_t$						
	1	2	3	4	5	6	7
$R^2$	0.615	0.451	0.643	0.759	0.725	0.630	0.572



**Table 2.** Status of the required time in locations.

Location	Time of Concentration
Borçka	3
Hopa	2
Şavşat	3
Arhavi	3
Murgul	1
Yusufeli	7
Artvin	5

**4. Conclusion**

Recent studies indicate that increased flood risks in various regions are significantly influenced by changes in rainfall intensity [47, 48], global warming, and land modifications. Variations in rainfall intensity or amount are leading to more frequent floods in coastal cities [49, 50], which are also affected by rising sea levels and a higher incidence of tropical storms due to global warming [51, 52]. Additionally, land modifications at various scales exacerbate vulnerability to flood risks; for example, urbanization and deforestation heighten flood hazards in smaller catchments [53, 54]. The effects of climate change on this study not only increase the frequency and intensity of flood events but also complicate their prediction. Changing climatic conditions create uncertainties in rainfall patterns, which can affect the accuracy of forecasts. Therefore, it is important to consider the impacts of climate change in the accurate assessment and prediction of flood risks. Climate change, including atmospheric warming, further alters the frequency and intensity of extreme hydrological events, thereby amplifying flood risk [55]. Baudhanwala et al. [56] emphasized that, in light of the increasing impacts of these events, the complex interaction between rainfall characteristics and flood dynamics has become an important area of research.

In Turkey, studies on flash-flood related events have demonstrated an increase in the number of disasters attributed to rainfall [57, 58, 59, 39-60]. Specifically, orographic rains, which occur when steady air masses from northern and Western Europe pass over the Black Sea [61], play a significant role in the frequent occurrence of flood events in the Black Sea Region. For example, on 24 August 2015, flash floods in the city of Artvin resulted in severe losses to both life and property [39]. Similarly, during the flood disaster on November 11–12, 2015, high losses of life and property were reported, especially in Borçka, Murgul, Arhavi, and Hopa. Artvin has been affected by flooding events due to heavy rainfall in several instances: in July 2018 in Arhavi, July 2020 in Yusufeli, July 2021 in Arhavi, September 2022 in Arhavi, and in October 2023 in Arhavi, Borçka, and Hopa regions. Additionally, in July 2024, torrential rains in Yusufeli district caused flash floods in the morning hours in Esendal village. Flood events occurred during midsummer and autumn, when the amount of rainfall increased. This situation demonstrates that rainfall is the most significant factor affecting flood events. Akinci [62] also emphasized in his landslide susceptibility study conducted in the Artvin study area that landslides are most common during these months. Mehda et al. [63] and

Kantharia et al. [64] emphasized the necessity of rainfall data for flood forecasting in their studies. In this study, it is assumed that the meteorological data from 2009 to 2016 accurately reflects the rainfall patterns in the Eastern Black Sea Region, particularly in Artvin. This assumption is critical for the model's ability to predict future flood events based on historical data. Furthermore, it is posited that the ANN method can effectively capture the complex relationships between rainfall and runoff values, as well as the occurrence of floods.

The topographic and land use spatial characteristics of Artvin are significant factors influencing flood events in the region. Turgut and Turgut [40] reported that elevation values in Artvin range from the lowest in the Çoruh riverbed to up to 3.400 m in mountainous areas. They noted that areas within the 1.400-1.750 m elevation range represent the largest portion of the city, accounting for 20.1%, while areas within the 3.100-3.500 m elevation range correspond to the smallest areas. Steep terrain is common, with 42% of the city having slopes greater than 45% [40]. This situation demonstrates that the high mountainous terrain and rugged topography play a decisive role in how rainfall moves across the land surface and how water accumulates. According to Coordination of Information on the Environment (CORINE) 2018 land cover data, Artvin consists of bare rocks (3%), plant change areas (9%), agricultural land (16%), forests (30%), and natural grasslands (33%) [65]. Among these land cover types, the lack of vegetation cover and the potential of agricultural lands to accelerate surface water runoff contribute to an increased risk of flooding in Artvin. Beyond rainfall, topography, and land use, Artvin's geomorphological and lithological conditions, soil characteristics, humidity, and vegetation contribute to the frequent occurrence of flood events in the area. Given these conditions, it has become crucial to implement necessary measures to minimize damage from floods. The use of the ANN method in this study is important because it provides valuable information about potential floods, especially in residential areas, as it can quickly respond to rapid changes in rainfall [5, 7, 66, 67, 68-69]. Gunduz and Zeybekoglu [70] emphasized the importance of evaluations within the scope of modern disaster management approach for identifying risks and hazards, and for taking all necessary precautions. Thus, it can ensure that technical, legal and managerial precautions are taken in order to deal with the possible rapid flood disasters, with minimum damage and physical losses. In this case, the emergency measures that can be taken for the flood are better planned and applicable [71]. Policymakers can use this information to create targeted disaster preparedness plans, allocate resources effectively, and implement community-based interventions that enhance local resilience. ANN models can give a flood warning even a day before if enough accurate prediction models can be provided. Achieving a sufficiently accurate flood model ensures the emergency measures, which can be taken for floods, to be better planned and feasible. This will help the country managers to produce healthy policies and contribute to the national economy. In recent years, considering the

increasing prevalence of hazardous events (floods, droughts, soil erosion, and earthquakes), it is clear that such models are crucial for reducing loss of life and the socioeconomic impacts of these hazards [72].

Ibarreche et al. [73] introduce an early warning system for flash floods implemented in the Colima region of Mexico. The system sends email notifications to users with access to the system and aims to provide critical real-time information about flash flood events, giving people the minutes needed for evacuation before the event occurs. A concentration time of 3 to 5 hours has been determined. This duration demonstrates that the system's flood risk predictions and the time available for taking necessary measures are adequate. Ghanbari et al. [74] have developed an effective and highly accurate flood warning system for short-term predictions by integrating internet technologies, artificial intelligence, and hydraulic modeling methods in the Behesht-Abad watershed in Chaharmahal and Bakhtiari province, Iran. They have demonstrated the system's effectiveness in both flow predictions and spatial flood risk management.

The estimation flow values for the selected locations (except for Hopa) in this study increased above the threshold value after 20m<sup>3</sup>/h. When the results were evaluated, the time of concentration of 3 to 5 hours was chosen as the appropriate time period. This concentration time is consistent with the results of Ibarreche et al. [73]. The time calculated in this study is sufficient to take necessary measures. In the literature, the time required for effective preparation in case of flash flooding is given as approximately 2 hours [27, 28, 29-73]. In addition, the most important advantage of the ANN method is that it can accomplish with a small number of variables and information about hydrology which is necessary for modelling the flood dynamics. A similar study was conducted by Dtissibe et al. [75]. They developed an ANN model for flood forecasting using flow data as input and output variables. The model has a good generalization capacity and is able to successfully predict flood peaks with a 1-hour forecasting horizon, demonstrating good performance with low prediction errors. The researchers indicated that the model is an effective and reliable method for flood forecasting.

This study has developed an important model for flood forecasting in the Artvin region, and the results obtained provide a valuable foundation for future research. The use of the ANN method demonstrates an effective and valid approach to predicting flash flood events. In particular, the model's ability to consider complex dynamics such as climate change and the effects of precipitation is crucial for accurately assessing flood risks. In the study, the rationale for selecting a duration of 1-7 hours is that this time frame is critical for flood predictions. During this period, sudden rainfall and related hydrological events can be observed, enhancing the effectiveness of early warning systems. Additionally, the literature generally indicates that this range is necessary for effective preparation. Therefore, the study aimed to shape emergency response plans more effectively. However, there are some limitations to this study. Firstly, the meteorological data used only covers the years 2009–2016, which may impose constraints on the analysis of long-term trends. Although the model's

prediction error remains at a certain level, the accuracy of predictions may be adversely affected by sudden and extreme weather conditions. Additionally, since only daily average rainfall data was used in the study, the exclusion of other climatic factors, such as temperature and wind speed, may narrow the scope of the results. These findings may contribute to the development of more effective flood management strategies in the region.

Floods are one of the worst environmental disasters that affect both civilization and the environment on a global scale. They destroy not only social and environmental assets but also human lives [76]. For this reason, the development of such models is valuable for reducing the economic and environmental impacts of floods. With this study, it has been shown that ANN can be used as a valid and effective approach to predict flash flood events. In conclusion, by integrating these advanced predictive tools into disaster management strategies, communities can enhance their preparedness and resilience against future flood risks.

### Acknowledgement

This work was supported by a research grant from Ankara University Research Council (#17B0649001 to O. A.).

### Author contributions

**Olgu Aydın:** Conceptualization, Methodology, Software, Field study, Writing-Original draft preparation, Project administration. **Nussaibah Begum Raja:** Data curation, Methodology, Software, Visualization, Writing-Reviewing and Editing.

### Conflicts of interest

The authors declare no conflicts of interest.

### References

1. NatCatSERVICE. (2016). [Online] Available from: <https://www.munichre.com/> [Accessed 20 February 2019]
2. EM-DATI. (2016). The international disasters database [Online] Available from: <http://www.emdat.be/> [Accessed 20 February 2019]
3. Mahmood, S., & Rani, R. (2022). People-centric geo-spatial exposure and damage assessment of 2014 flood in lower Chenab Basin, upper Indus Plain in Pakistan. *Natural Hazards*, 111(3), 3053–3069. <https://doi.org/10.1007/s11069-021-05167-w>
4. Manizabayo, P., Ngwijabagabo, H., Nzayisenga, I., Nzamwita, S., Amani, L., Uwitonze, E., & Gilbert, K. M. (2024). Assessment of flood susceptibility utilizing remote sensing and geographic information systems: A case study of Mpazi sub-catchment in the city of Kigali. *Advance GIS*, 4(1), 31–41. e-ISSN:2822-7026
5. Campolo, M., Soldati, A., & Andreussi, P. (2003). Artificial neural network approach to flood forecasting in River Arno. *Hydrological Sciences Journal*, 48(3), 381–398. <https://doi.org/10.1623/hysj.48.3.381.45286>

6. Ashley, S. T., & Ashley, W. S. (2008). Flood fatalities in the United States. *American Meteorological Society*, 47(3), 805–818. <http://doi.org/10.1175/2007JAMC1611.1>
7. EsiefarienrheBukohwo, M., & OfikwuEne, P. (2018). Flood prediction in Nigeria using artificial neural network. *American Journal of Engineering Research (AJER)*, 7(9), 15–21. e-ISSN: 2320-0847
8. Güner, İ., & Uçar, İ. (2021). The inventory of flood disasters in Turkey. *5th International Environmental Conference "Impact of Climate Change, Water and Energy on Sustainable Environmental Resources Management" (CWESM-2021)*, Krenia North Cyprus.
9. Tortumlu, M., & Altuncı, Y. A. (2024). Analysis of flood disasters in Türkiye and their effects on health. *Anatolian Journal of Emergency Medicine*, 7(2), 74–80. <https://doi.org/10.54996/anatolianjem.1376324>
10. Boé, J., Somot, S., Corre, L., & Nabat, P. (2020). Large discrepancies in summer climate change over Europe as projected by global and regional climate models: causes and consequences. *Climate Dynamics*, 54(5–6), 2981–3002. <http://doi.org/10.1007/s00382-020-05153-1>
11. Borga, M., Gaume, E., Creutin, J. D., & Marchi, L. (2008). Surveying flash flood response: gauging the ungauged extremes. *Hydrological Processes*, 22(18), 3883–3885. <https://doi.org/10.1002/hyp.7111>
12. Guéro, P. (2006). Rainfall analysis and flood hydrograph determination in the Munster Blackwater Catchment. (A Thesis of Degree of Master). Department of Civil and Environmental Engineering, University College Cork.
13. Sun, D., Zhang, D., & Cheng, X. (2012). Framework of national non-structural measures for flash flood disaster prevention in China. *Water*, 4(1), 272–282. <https://doi.org/10.3390/w4010272>
14. Yang, T. H., Yang, S. C., Ho, J. Y., Lin, G. F., Hwang, G. D., & Lee, C. S. (2015). Flash flood warnings using the ensemble rainfall forecasting technique: A case study on forecasting floods in Taiwan caused by typhoons. *Journal of Hydrology*, 520, 367–378. <http://dx.doi.org/10.1016/j.jhydrol.2014.11.028>
15. Carpenter, T. M., Sperflage, J. A., Geogakakos, K. P., Sweeney, T., & Fread, D. L. (1999). National threshold runoff estimation utilizing GIS in support of operational flash flood warning systems. *Journal of Hydrology*, 224, 21–44. [https://doi.org/10.1016/S0022-1694\(99\)00115-8](https://doi.org/10.1016/S0022-1694(99)00115-8)
16. Prasantha-Hapuarachchi, H. A., & Wang, Q. J. (2008). A review of methods and systems available for flash flood forecasting. Report for the Bureau of Meteorology, Australia. <http://doi.org/10.4225/08/58542bbf33ce7>
17. Kamali, M. A., & Ma'ady, M. N. P. (2024). IoT-based flood disaster early detection system using hybrid fuzzy logic and neural networks. *Telecommunication Computing Electronics and Control*, 22(4), 976–984. <http://doi.org/10.12928/TELKOMNIKA.v22i4.25868>
18. Gaume, E., Bain, V., Bernardara, P., Newinger, O., Barbuc, M., Bateman, A., Blaskovicova, L., Bloschl, G., Borga, M., Dumitrescu, A., Daliakopoulos, I., Garcia, J., Irimescu, A., Kohnova, S., Koutroulis, A., Marchi, L., Matreata, S., Medina, V., Preciso, E., Sempere-Torres, D., Stancalie, G., Szolgay, J., Tsanis, I., Velasco, D., & Viglione, A. (2009). A compilation of data on European flash floods. *Journal of Hydrology*, 367(1–2), 70–78. <https://doi.org/10.1016/j.jhydrol.2008.12.028>
19. Marchi, L., Borga, M., Preciso, E., & Gaume, E. (2010). Characterisation of selected extreme flash floods in Europe and implications for flood risk management. *Journal of Hydrology*, 394(1–2), 118–133. <https://doi.org/10.1016/j.jhydrol.2010.07.017>
20. Ahmad, M., Al Mehedi, M. A., Yazdan, M. M. S., & Kumar, R. (2022). Development of machine learning flood model using artificial neural network (ANN) at Var River. *Liquids*, 2, 147–160. <https://doi.org/10.3390/liquids2030010>
21. Saikh, N. I., & Mondal, P. (2023). GIS-based machine learning algorithm for flood susceptibility analysis in the Pagla river basin, Eastern India. *Natural Hazards Research*, 3, 420–436. <https://doi.org/10.1016/j.nhres.2023.05.004>
22. Sharma, S., & Kumari, S. (2024). Comparison of machine learning models for flood forecasting in the Mahanadi River Basin, India. *Journal of Water and Climate Change*, 15(4), 1629–1652. <http://doi.org/10.2166/wcc.2024.517>
23. Çubukçu, E. A., Demir, V., & Sevimli, M. F. (2023). Modeling of annual maximum flows with geographic data components and artificial neural networks. *International Journal of Engineering and Geosciences*, 8(2), 200–211. <http://doi.org/10.26833/ijeg.1125412>
24. Byaruhanga, N., Kibirige, D., Gokool, S., & Mkhonta, G. (2024). Evolution of flood prediction and forecasting models for flood early warning systems: A scoping review. *Water*, 16(13), 1763, 1–29. <https://doi.org/10.3390/w16131763>
25. Varoonchotikul, P. (2003). Flood forecasting using artificial neural networks. CRC Press. ISBN 9789058096319
26. Campolo, M., Soldati, A., & Andreussi, P. (1999). Forecasting river flow rate during low-flow periods using neural networks. *Water Resources Research*, 35(11), 3547–3552. <http://doi.org/10.1029/1999WR900205>
27. Artigue, G., Johannet, A., Borrell, V., & Pistre, S. (2012). Flash flood forecasting in poorly gauged basins using neural networks: Case study of the Gardon de Mialet Basin (Southern France). *Natural Hazards and Earth System Sciences*, 12(11), 3307–3324. <https://doi.org/10.5194/nhess-12-3307-2012>
28. Cools, J., Vanderkimpen, P., El Afandi, G., Abdelkhalek, A., Fockedey, S., El Sammany, M., Abdallah, G., El Bihery, M., Bauwens, W., & Huygens, M. (2012). An early warning system for flash floods in hyper-arid Egypt. *Natural Hazards and Earth System Sciences*, 12(2), 443–457. <https://doi.org/10.5194/nhess-12-443-2012>
29. Raja, N. B., & Aydin, O. (2017). New approaches to flash flood forecasting in the Mediterranean Region. Lambert Academic Publishing, Saarbrücken, Germany. ISBN-10:3330321342

30. Lamsal, R., & Vijay Kumar, T. V. (2020). Artificial Intelligence and Early Warning Systems. In: Lamsal, R., & Vijay Kumar, T. V. (Ed). AI and Robotics in Disaster Studies. Palgrave Macmillan, Singapore. [http://doi.org/10.1007/978-981-15-4291-6\\_2](http://doi.org/10.1007/978-981-15-4291-6_2)
31. Stephens, E., & Cloke, H. (2014). Improving flood forecasts for better flood preparedness in the UK (and beyond). *The Geographical Journal*, 180(4), 310–316. <https://www.jstor.org/stable/43870924>
32. Aydin, O., & Raja, N. B. (2020). Spatial-temporal analysis of precipitation characteristics in Artvin, Turkey. *Theoretical and Applied Climatology*, 142(5), 729–741. <http://doi.org/10.1007/s00704-020-03346-6>
33. Zeybekoglu, U., & Keskin, A. U. (2020). Detrended fluctuation analyses of rainfall intensities: A case study. *International Journal of Global Warming*, 21(2), 141–154. <http://doi.org/10.1504/IJGW.2020.108175>
34. Özalp Yavuz, A., Akıncı, H., & Temuçin, S. (2013). Artvin ili arazisinin topografik ve bazı fiziksel özelliklerinin tespiti ve bu özelliklerin arazi örtüsü ile ilişkisinin incelenmesi. *Artvin Çoruh Üniversitesi Orman Fakültesi Dergisi*. 14(2), 292–309. ISSN:2146-1880
35. Ketin, İ. (1949). Artvin bölgesinin jeolojik etüdü hakkında memuar. Ankara: MTA Enstitü Yayınları.
36. Ketin, İ. (1954). Artvin bölgesinin jeolojik etüdü hakkında memuar. Ankara: MTA Rapor.
37. Gattinger, T. E., Erentöz, C., İhsan, K. (1962). Türkiye jeoloji haritası Trabzon-1.500.000 ölçekli-explonatory text of geological map of Turkey. *Modern Tetkik ve Arama Enstitüsü Yayınları*, Ankara.
38. Köse, N., & Güner, H. T. (2012). The effect of temperature and precipitation on the intra-annual radial growth of *Fagus orientalis* Lipsky in Artvin, Turkey. *Journal of Agriculture and Forestry*, 36(4), 501–509. <http://doi.org/10.3906/tar-1109-4>
39. Baltacı, H. (2017). Meteorological analysis of flash floods in Artvin (NE Turkey) on 24 August 2015. *Natural Hazards and Earth System Sciences*, 17(7), 1221–1230. <https://doi.org/10.5194/nhess-17-1221>
40. Turgut, H., & Turgut, B. (2022). The effects of landforms and climate on NDVI in Artvin, Turkey. *Eco Mont-Journal on Protected Mountain Areas Research*, 14(2), 24–36. <http://doi.org/10.1553/eco.mont-14-2s24>
41. Pebesma, E. J., & Wesseling, C. G. (1998). Gstat, a program for geostatistical modelling, prediction and simulation. *Computers&Geosciences*, 24(1), 17–31. [https://doi.org/10.1016/S0098-3004\(97\)00082-4](https://doi.org/10.1016/S0098-3004(97)00082-4)
42. Pebesma, E. J. (2004). Multivariable geostatistics in S: the gstat package. *Computer&Geosciences*, 30, 683–691. <http://doi.org/10.1016/j.cageo.2004.03.012>
43. Bivand, R. S., Pebesma, E., & Gómez-Rubio, V. (2008). Applied spatial data analysis with R (use R!). 1. Edition, Springer, London. <http://doi.org/10.1007/978-0-387-78171-6>
44. Thompson, D. (2006). The rational method. *Engineering, Environmental Science*, [http://doi.org/10.1007/978-3-642-41714-6\\_180527](http://doi.org/10.1007/978-3-642-41714-6_180527)
45. Maier, H. R., Jain, A., Dandy, G. C., & Sudheer, K. P. (2010). Methods used for the development of neural networks for the prediction of water resource variables in river systems: current status and future directions. *Environmental Modelling Software*, 25(8), 891–909. <https://doi.org/10.1016/j.envsoft.2010.02.003>
46. Krenker, A., Bešter, J., & Kos, A. (2011). Introduction to the Artificial Neural Networks. In: Suzuki, K. (Ed). Artificial Neural Networks-Methodological Advances and Biomedical Applications. InTech., Croatia. <http://doi.org/10.5772/15751>
47. Chaudhari, R. P., Thorat, S. R., Mehta, D. J., Waikhom, S. I., Yadav, V. G., & Kumar, V. (2024). Comparison of soft-computing techniques: Data-driven models for flood forecasting. *AIMS Environmental Science*, 11(5), 741–758. <http://doi.org/10.3934/environsci.2024037>
48. Mangukiya, N. K., Mehta, D. J., & Jariwala, R. (2022). Flood frequency analysis and inundation mapping for lower Narmada basin, India. *Water Practice & Technology*, 17(2), 612–622. <http://doi.org/10.2166/wpt.2022.009>
49. Patel, S., Gohil, M., Pathan, F., Mehta, D., & Waikhom, S. (2024). Assessment of flood risk and its mapping in Navsari District, Gujarat. *Iranian Journal of Science and Technology, Transactions of Civil Engineering*, 48(2), 1021–1028. <https://doi.org/10.1007/s40996-023-01225-4>
50. Mehta, D. J., Eslamian, S., & Prajapati, K. (2022). Flood modelling for a data-scare semi-arid region using 1-D hydrodynamic model: A case study of Navsari Region. *Modeling Earth Systems and Environment*, 8(2), 2675–2685. <https://doi.org/10.1007/s40808-021-01259-5>
51. Chang, H., & Franczyk, J. J. (2008). Climate change, land-use change, and floods: Toward an integrated assessment. *Geography Compass*, 2(5), 1549–1579. <http://doi.org/10.1111/j.1749-8198.2008.00136.x>
52. Andersen, T. K., & Marshall Shepherd, J. (2013). Floods in a changing climate. *Geography Compass*, 7(2). <http://doi.org/10.1111/gec3.12025>
53. Llasat, M. C. (2021). Floods evolution in the Mediterranean region in a context of climate and environmental change. *Geographical Research Letters*, 47(1), 13–32. <https://doi.org/10.18172/cig.4897>
54. Blöschl, G. (2022). Three hypotheses on changing river flood hazards. *Hydrology and Earth System Sciences*, 26(19), 5015–5033. <http://doi.org/10.5194/hess-26-5015-2022>
55. Huang, X., Yin, J., Slater, L. J., & Liu, P. (2024). Global projection of flood risk with a bivariate framework under 1.5–3.0°C warming levels. *Earth's Future*, 12(4), 1–19. <http://doi.org/10.1029/2023EF004312>
56. Baudhanwala, D., Mehta, D., Zoysa, S., & Rathnayake, U. (2024). Rainfall intensity-duration-frequency relationships: a robust foundation for urban decision-making and flood management: A case study. *Journal of Environmental Informatics Letters*, 11(2), 101–108. <http://doi.org/10.3808/jeil.202400131>
57. Kömüşçü, A. Ü., Erkan, A., & Çelik, S. (1998). Analysis of meteorological and terrain features leading to the İzmir Flash Flood, 3–4 November 1995. *Natural*

- Hazards*, 18, 1–25. <http://doi.org/10.1023/A:1008078920113>
58. Kotroni, V., Lagouvardos, E., Defer, S., Dietrich, F., Porcù, C., Medaglia, C. M., & Demirtas, M. (2006). The Antalya 5 December 2002 storm: Observations and model analysis. *Journal of Applied Meteorology Climatology*, 45, 576–590. <https://doi.org/10.1175/JAM2347.1>
59. Kömüşçü, A. Ü., & Çelik, S. (2013). Analysis of the Marmara flood in Turkey, 7–10 September 2009: An assessment from hydrometeorological perspective. *Natural Hazards*, 66(2), 781–808. <http://doi.org/10.1007/s11069-012-0521-x>
60. Baltacı, H. (2018). 18 Temmuz 2017 tarihinde İstanbul'da meydana gelen sel olayının meteorolojik analizi. *Marmara Fen Bilimleri Dergisi*, 30(1), 55–60. <https://doi.org/10.7240/marufbd.397544>
61. Özcan, E. (2006). Sel olayı ve Türkiye. *Gazi Üniversitesi Gazi Eğitim Fakültesi Dergisi*, 26(1), 35–50.
62. Akinci, H. (2022). Assessment of rainfall-induced landslide susceptibility in Artvin, Turkey using machine learning techniques. *Journal of African Earth Sciences*, 191, 1–17. <http://doi.org/10.1016/j.jafrearsci.2022.104535>
63. Mehta, D., Dhabuwala, J., Yadav, S. M., Kumar, V., & Azamathulla, H. M. (2023). Improving flood forecasting in Narmada river basin using hierarchical clustering and hydrological modelling. *Results in Engineering*, 20, 101571, 1–13. <https://doi.org/10.1016/j.rineng.2023.101571>
64. Kantharia, V., Mehta, D., Kumar, V., Shaikh, M. P., & Jha, S. (2024). Rainfall–runoff modeling using an adaptive neuro-fuzzy inference system considering soil moisture for the Damanganga Basin. *Journal of Water and Climate Change*, 15(5), 2518–2531. <https://doi.org/10.2166/wcc.2024.143>
65. Akinci, H., Zeybek, M. (2021). Comparing classical statistic and machine learning models in landslide susceptibility mapping in Ardanuc (Artvin), Turkey. *Natural Hazards*, 108, 1515–1543. <https://doi.org/10.1007/s11069-021-04743-4>
66. Dawson, C. W., & Wilby, R. (1998). An artificial neural network approach to rainfall-runoff modelling. *Hydrological Sciences*, 43(1), 47–66. <http://doi.org/10.1080/02626669809492102>
67. Kalteh, A. M. (2007). Rainfall-runoff modelling using artificial neural networks (ANNs). (Thesis). Department of Water Resources Engineering, Lund Institute of Technology, Lund University, Sweden.
68. Nkoana, R. (2011). Artificial neural network modelling of flood prediction and early warning. [Doctoral Thesis (compilation), Division of Water Resources Engineering]. Department of Water Resources Engineering, Lund Institute of Technology, Lund University.
69. Elsafi, S. H. (2014). Artificial neural networks (ANNs) for flood forecasting at Dongola Station in the River Nile, Sudan. *Alexandria Engineering Journal*, 53(3), 655–662. <https://doi.org/10.1016/j.aej.2014.06.010>
70. Gunduz, F., & Zeybekoglu, U. (2024). Analysis of temperature and rainfall series of Hirfanli Dam Basin by mann kendall, spearman's rho and innovative trend analysis. *Turkish Journal of Engineering*, 8(1), 11–19. <http://doi.org/10.31127/tuje.1177522>
71. Demir, V., & Keskin, A. Ü. (2022). Yeterince akım ölçümü olmayan nehirlerde taşkın debisinin hesaplanması ve taşkın modellemesi (Samsun, Mert Irmağı örneği). *Geomatik*, 7(2), 149–162. <http://doi.org/10.29128/geomatik.918502>
72. Gohil, M., Mehta, D., & Shaikh, M. (2024). An integration of geospatial and fuzzy-logic techniques for multi-hazard mapping. *Results in Engineering*, 21, 101758, 1–22. <https://doi.org/10.1016/j.rineng.2024.101758>
73. Ibarreche, J., Aquino, R., Edwards, R. M., Rangel, V., Pérez, I., Martínez, M., Castellanos, E., Álvarez, E., Jimenez, S., Rentería, R., Edwards, A., & Álvarez, O. (2020). Flash flood early warning system in Colima, Mexico. *Sensors*, 20(18), 1–26. <http://doi.org/doi:10.3390/s20185231>
74. Ghanbari, A., Tahmasebipour, N., Zeinivand, H., Heidari, M. I. A., & Abdollahi, S. (2024). Flood warning system using internet of things, artificial intelligence and hydraulic modeling (case study: Behesht-Abad Watershed, Iran). *Acta Geophysica*, 72, 2815–2829. <https://doi.org/10.1007/s11600-023-01174-6>
75. Dtissibe, F. Y., Ari, A. A. A., Titouna, C., Thiare, O., & Gueroui, A. M. (2020). Flood forecasting based on an artificial neural network. *Natural Hazards*, 104, 1211–1237. <https://doi.org/10.1007/s11069-020-04211-5>
76. Gohil, M., Mehta, D., & Shaikh, M. (2024). An integration of geospatial and fuzzy-logic techniques for flood-hazard mapping. *Journal of Earth System Science*, 133(2), 80. <https://doi.org/10.1007/s12040-024-02288-1>

